ACCOUNTS
of chemical research

Composition-Tunable Alloyed Semiconductor Nanocrystals

MICHELLE D. REGULACIO[†] AND MING-YONG HAN[*,†,‡]

[†]*Institute of Materials Research and Engineering, A*STAR (Agency for Science, Technology and Research), 3 Research Link, Singapore 117602, and* [‡]*Division of Bioengineering, National University of Singapore, Singapore 117576*

RECEIVED ON SEPTEMBER 17, 2009

CONSPECTUS

The ability to engineer the band gap energy of semiconductor nanocrystals has led to the development of nanomaterials with many new exciting properties and applications. Band gap engineering has thus proven to be an effective tool in the design of new nanocrystal-based semiconductor devices. As reported in numerous publications over the last three decades, tuning the size of nanocrystalline semiconductors is one way of adjusting the band gap energy. On the other hand, research on band gap engineering via control of nanocrystal composition, which is achieved by adjusting the constituent stoichiometries of alloyed semiconductors, is still in its infancy. In this Account, we summarize recent research on colloidal alloyed semiconductor nanocrystals that exhibit novel composition-tunable properties.

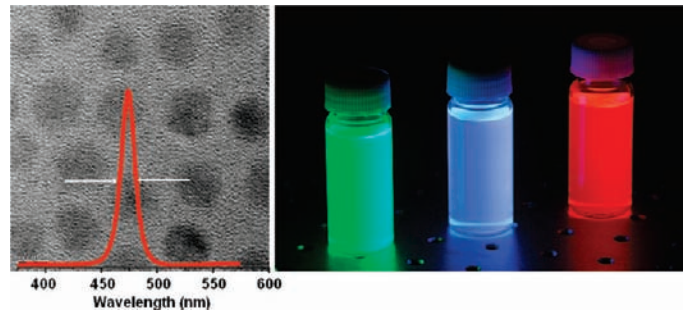

Alloying of two semiconductors at the nanometer scale produces materials that display properties distinct not only from the properties of their bulk counterparts but also from those of their parent semiconductors. As a result, alloyed nanocrystals possess additional properties that are composition-dependent aside from the properties that emerge due to quantum confinement effects. For example, although the size-dependent emission wavelength of the widely studied CdSe nanocrystals can be continuously tuned to cover almost the entire visible spectrum, the near-infrared (NIR) region is far outside its spectral range. By contrast, certain alloy compositions of nanocrystalline $CdSe_xTe_{1-x}$, an alloy of CdSe and CdTe, can efficiently emit light in the NIR spectral window. These NIR-emitting nanocrystals are potentially useful in several biomedical applications. In addition, highly stable nanocrystals formed by alloying CdSe with ZnSe (i.e., $Zn_xCd_{1-x}Se$) emit blue light with excellent efficiency, a property seldom achieved by the parent binary systems. As a result, these materials can be used in short-wavelength optoelectronic devices.

In the future, we foresee new discoveries related to these interesting nanoalloys. In particular, colloidal semiconductor nanoalloys that exhibit composition-dependent magnetic properties have yet to be reported. Further studies of the alloying mechanism are also needed to develop improved synthetic strategies for the preparation of these alloyed nanomaterials.

1. Introduction

The band gap energy, E_g, determines many of the semiconductor's properties, and because of this a great deal of interest has been given to band gap engineering as a powerful technique in the development of new semiconductor materials, particularly at the nanoscale. Due to quantum confinement, reducing the dimensions of a semiconductor to a size comparable to or smaller than its exciton Bohr radius effectively widens its energy gap. Thus, altering the nanocrystal size is one way of tuning the semiconductor band gap. Size-controlled syntheses of semiconductor nanocrystals (often referred to as quantum dots, QDs) that exhibit band-gap-dependent properties have been widely investigated.[1−3] These properties are

Published on the Web 03/10/2010 www.pubs.acs.org/acr
10.1021/ar900242r

FIGURE 1. Composition-tunable emission color of alloyed $Zn_xCd_{1-x}Se$ nanocrystals.

remarkably different from those of the corresponding bulk material and have given rise to a multitude of potential applications in a wide array of fields, which include optoelectronics, catalysis, photovoltaics, and biological imaging. However, in many particular applications, very small nanocrystals are necessary to achieve the desired properties and the instability of particles with extremely small diameter (<2 nm) poses a great problem. It has thus become a challenge to be able to tune the nanocrystal properties independent of their size.

Another means of tailoring the semiconductor band gap is by changing the particle composition via control of constituent stoichiometries. This can be achieved by creating a solid solution (i.e., an alloy) of two semiconductors with different energy gaps. An increase in band gap energy is generally observed with increasing content of the wider band gap semiconductor. This technique should not be confused with doping (i.e., the intentional introduction of impurity atoms into a semiconductor). While impurity doping is a process chemically related to alloying, it does not really shift the band gap of the host semiconductor but modifies the band structure by creating electronic energy levels (dopant states) within the band gap that allows for lower energy light emission.[4]

Our group has reported the preparation of composition-controlled alloyed semiconductor nanocrystals of superior quality by employing an effective high-temperature synthetic strategy. Our synthesized $Zn_xCd_{1-x}Se$ nanocrystals display composition-tunable emission color across the visible spectral window (Figure 1) and exhibit luminescence efficiencies that can rival those reported for the most often studied CdSe nanocrystals.[5] Moreover, these alloyed nanomaterials have shown interesting properties that are not observed in the simpler binary systems. In this Account, we focus our review on the synthesis, applications, and composition-tunable properties of colloidal alloyed semiconductor nanocrystals that have been reported over the past decade.

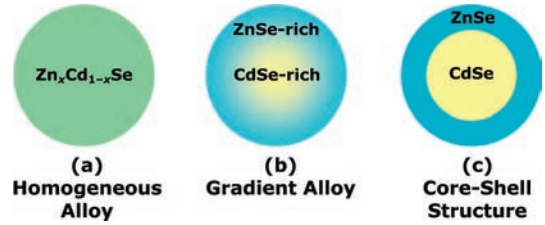

FIGURE 2. Schematic representation of spherical nanocrystals having a (a) homogeneous, (b) gradient, and (c) core−shell structure using ZnCdSe as example.

2. Classification of Alloyed Semiconductor Nanocrystals

Alloyed semiconductor nanocrystals can be classified as having (1) a uniform internal structure (i.e., homogeneous) or (2) a gradient internal structure, where the alloy composition varies in different parts of the nanocrystal. These are different from the core−shell structure, where a thin layer of a wider band gap semiconductor is grown on the surface of a core semiconductor. Figure 2 schematically shows the difference between nanocrystals having a homogeneous, gradient, and core−shell structure.

Depending on the number of component elements that constitute the alloy, they can be classified as either ternary (3 elements) or quarternary (4 elements). Ternary alloys are formed when the parents are two binary systems with either a common anion or cation. For instance, alloying of M′A and M″A produces $(M'A)_x(M''A)_{1-x}$ or simply $M'_xM''_{1-x}A$, where M′ and M″ are two different cations and A is the common anion. $Zn_xCd_{1-x}Se$ is an example of this type of alloy. Common cation alloyed composition, $MA'_xA''_{1-x}$, is formed through alloying of MA′ and MA″, where M is the common cation while A′ and A″ are two different anions. An example of which is CdS_xSe_{1-x}, an alloy of CdS and CdSe.

Alloying of two binary systems with no common elements produces quarternary alloys having the composition $M'_xM''_{1-x}A'_yA''_{1-y}$. Nanocrystals of this type of alloy have not been colloidally prepared until recently, with the synthesis of $Zn_xCd_{1-x}S_ySe_{1-y}$ QDs in paraffin liquid by Deng and co-workers.[6] Quarternary alloys can also form through alloying of ternary I−III−VI_2 semiconductors, also referred to as chalcopyrite materials. The most notable example of this is $CuIn_xGa_{1-x}Se_2$ (CIGS), which results from alloying $CuInSe_2$ and $CuGaSe_2$.[7] Alloying a ternary with a binary semiconductor can also yield a quartenary system as in the case of $(CuInS_2)_x(ZnS)_{1-x}$.[8]

3. Colloidal Synthesis

Alloyed semiconductor nanostructures have been prepared through synthetic approaches that involve solid-state reaction/

decomposition, thermal evaporation, and vapor deposition. The use of sol−gel process (with solid-state annealing as the final step) has also been demonstrated, particularly in the synthesis of $Mg_xZn_{1-x}O$ nanomaterials.[9] In this Account, we focus mainly on purely colloidal routes to alloyed semiconductor nanocrystals.

3.1. $Zn_xCd_{1-x}Se$. The widely used high-temperature rapid injection technique has been the most successful in producing colloidal nanocrystals of high monodispersity.[10] Our group has demonstrated the use of this approach in the preparation of high-quality homogeneous $Zn_xCd_{1-x}Se$ QDs.[5] The procedure involves the consecutive rapid injection of solutions of $ZnEt_2$ and TOP-Se into a hot solution of preprepared CdSe QDs in coordinating solvents. The composition was tuned by varying the molar ratio of the Zn and Cd precursors. The high monodispersity and crystallinity of the resulting nanocrystals are evident from their high-resolution transmission electron microscopy (HRTEM) images as shown in Figure 3 for 7.5 nm $Zn_{0.67}Cd_{0.33}Se$ QDs. The systematic shifting of the diffraction peaks toward larger angles as the Zn content increases (Figure 3) is indicative of the decrease in lattice parameter due to the smaller ionic radius of Zn relative to that of Cd and is consistent with Vegard's law. This rules out phase separation or separated nucleation of ZnSe nanocrystals and is an indication of homogeneous alloy formation. Synthesis of $Zn_xCd_{1-x}Se$ QDs from ZnSe seeds or preprepared ZnSe QDs has also been reported.[11,12] Recent works have demonstrated the synthesis of $Zn_xCd_{1-x}Se$ nanocrystals in aqueous solutions using aminothiols (e.g., glutathione and cysteine) as capping agents.[13,14] With this approach, the reaction is done at relatively low temperatures (<100 °C), makes use of less toxic Zn precursors (e.g., $ZnCl_2$), and can be easily scaled up for the commercial production of biocompatible nanoalloys. Meanwhile, inorganic capping has produced $Zn_xCd_{1-x}Se$ nanocrystals with enhanced stability.[15]

3.2. $Zn_xCd_{1-x}S$. Wang et al. have prepared nanocrystalline $Zn_xCd_{1-x}S$ via a chemical reduction route at room temperature.[16] Unfortunately, the nanocrystals obtained from this method exhibit very broad emission peaks. Through a one-step hot-injection approach, our group has produced highly crystalline and monodisperse homogeneous wurtzite $Zn_xCd_{1-x}S$ QDs with excellent emission properties.[17] The procedure involves the reaction of ZnO- and CdO-oleic acid complexes with sulfur at 300 °C in noncoordinating solvent. Meanwhile, Li et al. have demonstrated the utility of Zn(II) and Cd(II) ethylxanthate complexes as molecular precursors that thermally decompose in hot coordinating solvents at relatively low temperatures (180−210 °C) to produce homogeneous

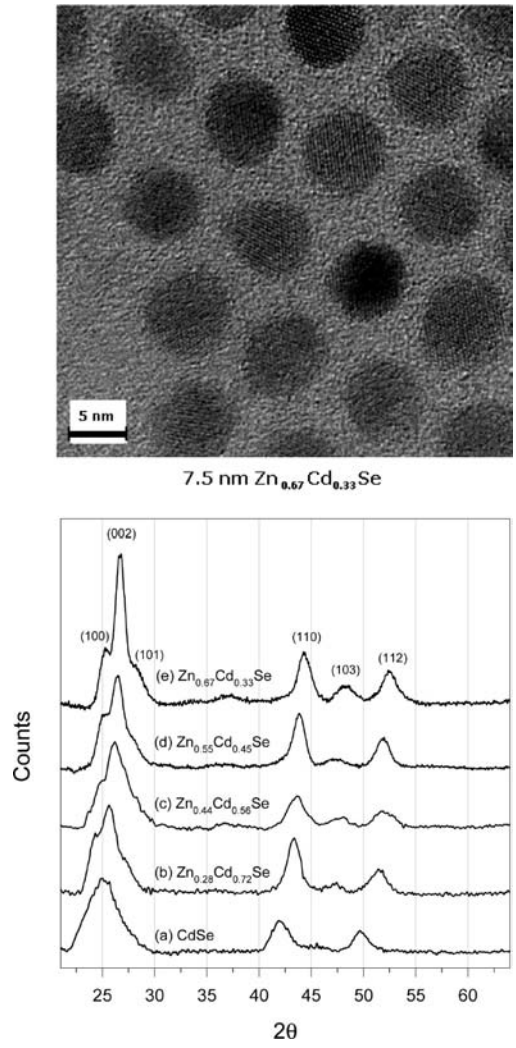

FIGURE 3. Top: HRTEM image of 7.5 nm $Zn_{0.67}Cd_{0.33}Se$ quantum dots. Bottom: PXRD patterns of $Zn_xCd_{1-x}Se$ quantum dots with Zn mole fractions of (a) 0, (b) 0.28, (c) 0.44, (d) 0.55, and (e) 0.67. Reprinted with permission from ref 5. Copyright 2003 American Chemical Society.

$Zn_xCd_{1-x}S$ nanocrystals.[18] Composition-induced shape and structural phase transitions were observed. Gradiently alloyed $Zn_xCd_{1-x}S$ QDs having a Cd-rich core and Zn-rich shell were synthesized via a noninjection one-pot approach by Ouyang and co-workers.[19] The resulting alloyed nanocrystals possess the cubic zinc-blende structure and were found to disobey Vegard's law implying a nonhomogeneous internal structure.

3.3. $CdE'_xE''_{1-x}$. Most of the synthetic methods used in the preparation of nanocrystalline $CdE'_xE''_{1-x}$ (where E′ and E″ are two different chalcogens) have been based on those of the binary cadmium chalcogenide nanocrystals. Generally, the procedure involves the rapid injection of a premixed solution containing stoichiometric amounts of the chalcogen precursors into a solution of Cd(II) precursor (usually CdO) in high-boiling coordinating and noncoordinating solvents at ∼300 °C

followed by the growth stage. This approach has been successful in producing alloyed nanocrystals of CdS_xSe_{1-x},[20] $CdSe_xTe_{1-x}$,[21] and CdS_xTe_{1-x}.[22] By controlling the amount of Cd used in the reaction, Bailey and Nie have synthesized $CdSe_xTe_{1-x}$ QDs having homogeneous (Cd-limited condition) and gradient (Cd-rich condition) internal structure.[21] Meanwhile, Gurusinghe et al. were able to prepare gradiently alloyed CdS_xTe_{1-x} nanocrystals by creating a 1−6 min delay between the S and Te injections.[22] Al-Salim et al. have used organic solvents with different coordinating properties in their synthesis of CdS_xSe_{1-x} nanocrystals.[23] Piven et al., on the other hand, reported the water-based synthesis of nanocrystalline $CdSe_xTe_{1-x}$.[24] More recently, Ouyang et al. have prepared homogeneously alloyed CdS_xSe_{1-x} nanocrystals via a noninjection route.[25] Inorganically passivated[26,27] and tetrapodal[28] $CdSe_xTe_{1-x}$ nanocrystals have also been made.

3.4. Other Ternary Alloys. Rogach et al. have synthesized gradiently alloyed $Cd_xHg_{1-x}Te$ QDs with CdTe-rich cores in water through subsequent layering of HgTe and CdTe onto preprepared thiol-stabilized CdTe QDs.[29] On the other hand, Sun et al. have prepared gradient $Cd_xHg_{1-x}Te$ QDs with HgTe-rich cores by utilizing the solubility difference between HgTe and CdTe in water.[30] To improve the stability and reduce the cytotoxicity of $Cd_xHg_{1-x}Te$ nanocrystals, surface passivation with an inorganic shell has been demonstrated.[31,32] The synthesis of glutathione-stabilized $Zn_xHg_{1-x}Se$ QDs in aqueous solution has also been reported.[33]

Reports on the synthesis of homogeneous Pb chalcogenide-based alloyed nanocrystals have been published very recently. Arachchige and Kanatzidis have prepared a series of $Pb_{1-x}Sn_xTe$ nanocrystals by reacting a mixture of Pb(II) oleate and $[(Me_3Si)_2N]_2Sn$ with TOP-Te at 150 °C.[34] Oleylamine was used as a stabilizer to facilitate the incorporation of Sn into the PbTe lattice. Energy-dispersive spectrometry (EDS) elemental maps show the even distribution of Sn in the entire PbTe lattice, confirming the structural homogeneity of the alloyed nanocrystals produced. Using a one-pot hot-injection approach, Ma et al. have synthesized monodisperse PbS_xSe_{1-x} nanocrystals.[35]

Nanocrystals of the III−V materials, when colloidally prepared, are usually inorganically coated due to their high instability to air. Kim et al. have reported the synthesis of colloidal QDs with a core−shell−shell structure consisting of an alloyed $InAs_xP_{1-x}$ core, an InP intermediate shell, and a ZnSe outer shell.[36] The alloyed core was found to have a gradient composition with increasing As content from the center to the edge of the dots. The InP shell increased the quantum yield of the material, whereas the ZnSe outer shell imparted stability in aqueous solutions.

3.5. Chalcopyrite Materials. $CuIn_xGa_{1-x}Se_2$ (CIGS) nanocrystals can be synthesized through a low-temperature colloidal route using methanol and pyridine as solvents.[37] However, the nanocrystals produced from this method are heavily aggregated. In contrast, using the high-temperature synthetic route, Tang et al. have been able to produce well-separated and nearly monodisperse CIGS nanocrystals.[7] This was achieved by rapid injection of a mixture containing the metal (Cu^{2+}, In^{3+} and Ga^{3+}) acetylacetonate complexes into a solution of Se in oleylamine at 250 °C. Using chloride salts as the metal source, Panthani et al. have also produced nanocrystalline CIGS.[38] Meanwhile, Guo et al. have synthesized $CuIn_xGa_{1-x}S_2$ by swift injection of a sulfur solution into an oleylamine solution of the metal chlorides at 225 °C.[39] Recently, Pan and co-workers have demostrated the synthesis of chalcopyrite-based quarternary alloyed nanocrystals using air-stable metal dithiocarbamate complexes.[8,40] The dithiocarbamate precursors were thermally decomposed in the presence of oleylamine to form the desired metal sulfides. Oleylamine not only reduced the decomposition temperature of the precursors but also minimized the reactivity difference between the precursors, thereby promoting the formation of a homogeneous internal structure.

4. Alloying Studies

A detailed understanding of the alloying mechanism is essential in developing better synthetic strategies for producing these alloyed nanomaterials. However, reports on these nanoalloys rarely include analysis of the alloying process. In our study of the alloying mechanism in the formation of homogeneously alloyed $Zn_xCd_{1-x}Se$ QDs, we observed that temperature plays an important role in the alloying process.[5] With our synthetic strategy (i.e., growth from preprepared CdSe QDs), CdSe−ZnSe core−shell structure is formed initially, but the high reaction temperature rapidly transforms it into the alloyed structure. The process of transforming the core−shell into the alloyed structure was studied by measuring the change in the emission maximum as a function of temperature. As seen in Figure 4a, the core−shell structure is retained below 270 °C, but it rapidly evolves into an alloy between 270 and 290 °C as evidenced by the significant blue shift in the emission maximum. Since the alloying process starts to occur at ∼270 °C, this is taken as the "alloying point". Sung et al. have studied the kinetics of this transformation process and concluded that the mechanism involves the dissociation

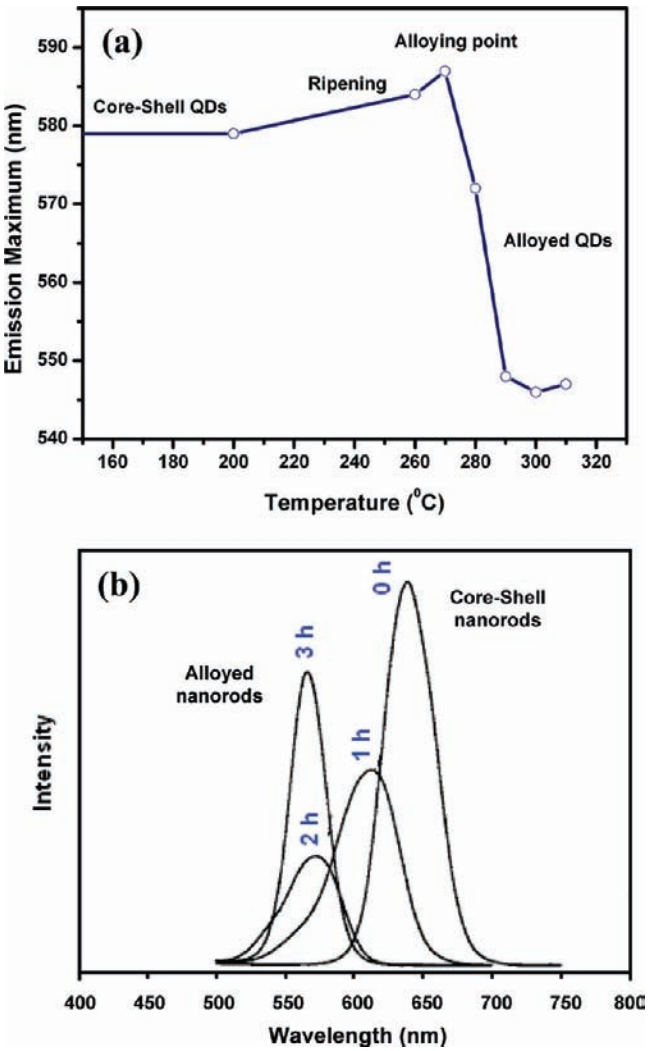

FIGURE 4. Alloying studies of the transformation from core−shell CdSe−ZnSe to alloyed $Zn_xCd_{1-x}Se$ by monitoring the evolution of the emission spectra under heat treatment at (a) different temperatures for 10 min each (Adapted with permission from ref 5. Copyright 2003 American Chemical Society) and (b) different heating times at 270 °C (Reprinted with permission from ref 42. Copyright 2006, American Institute of Physics).

of bonds between Zn^{2+} and Se^{2-} ions and the diffusion of Zn^{2+} into the CdSe matrices.[41] Heat treatment at higher temperatures results in a higher rate of alloy formation, which is possibly due to the increased mobility of diffusing ions. Lee et al. studied the effect of heating time in their thermal treatment of CdSe−ZnSe core−shell nanorods at 270 °C, and the evolution of the emission spectra with time is shown in Figure 4b.[42] The blue-shifting of the emission maximum with increasing heating time results from the progressive incorporation of the wider band gap ZnSe into the CdSe core. The broadening and skewing of the emission peak at shorter heating times are attributed to compositional disorder as the core−shell structure is still in the process of transforming into a homogeneous alloyed structure.

When $Zn_xCd_{1-x}Se$ QDs are prepared from ZnSe nuclei or ZnSe QDs, a red-shift in the emission maximum was observed during the alloying stage as a result of the decrease in band gap energy as Cd^{2+} is progressively incorporated into the ZnSe lattice.[11,12] Alloy formation occurred at temperatures lower than the alloying point for the CdSe-seeded growth, which implies that cation exchange reaction between ZnSe nanocrystals and Cd^{2+} is more favored than that between CdSe and Zn^{2+}. This is attributed to the much lower bond dissociation energy of Zn−Se (136 kJ mol^{-1}) relative to Cd−Se (310 kJ mol^{-1}).

Based on their kinetic analysis and experimental studies, Bailey and Nie have shown that the internal structure of $CdSe_xTe_{1-x}$ QDs can be controlled by the amount of Cd used in the reaction.[21] Under rapid nucleation and growth conditions, Te is more reactive than Se toward Cd, and because of this the CdTe growth rate is approximately double that of CdSe. If the amount of chalcogen precursors is in large excess of the Cd concentration (Cd-limited condition), the effect of the difference in chalcogen reactivity is minimized, and this consequently leads to an alloy with homogeneous internal structure. On the other hand, under Cd-rich conditions, the faster CdTe growth rate results in a gradient alloy structure with decreasing Te content from the core to the surface (i.e., CdTe-rich core).

In their synthesis of gradient $Cd_xHg_{1-x}Te$ QDs, Sun et al. made use of the difference in solubility between HgTe and CdTe in water.[30] Using equal concentrations of Cd and Hg, HgTe nucleates at a faster rate than CdTe due to the much lower solubility of HgTe in water. Thus, the nanocrystals that initially form are mostly made of HgTe, and CdTe deposition becomes dominant only when Hg is depleted in the reaction mixture. This yielded alloyed nanocrystals with Hg content decreasing from the core to the surface.

5. Properties and Applications

Alloying of two semiconductors produces materials with characteristics distinct from those of the parent semiconductors. Some of the interesting properties and potential applications of alloyed semiconductor nanocrystals are discussed below.

5.1. Optical Properties. Figure 5 shows the absorption and photoluminescence (PL) spectra measured from our nanocrystalline $Zn_xCd_{1-x}Se$ samples.[5] The systematic blue-shifting of the absorption onset and the emission maximum as the Zn content increases is due to the wider band gap of ZnSe relative to that of CdSe, and it is clearly indicative of the formation of the alloyed $Zn_xCd_{1-x}Se$ QDs rather than the parent binary systems or the core−shell structure. Similar to bulk

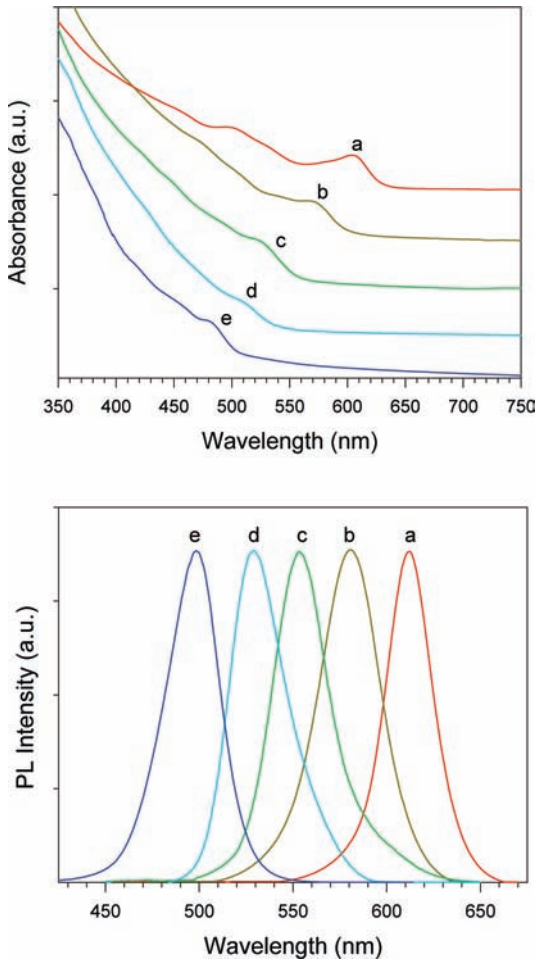

FIGURE 5. Absorption (top) and emission (bottom) spectra of $Zn_xCd_{1-x}Se$ quantum dots with Zn mole fractions of (a) 0, (b) 0.28, (c) 0.44, (d) 0.55, and (e) 0.67. Reproduced with permission from ref 5. Copyright 2003 American Chemical Society.

$Zn_xCd_{1-x}Se$ alloy, a very slight nonlinear relationship between the band gap energy and the composition, known as "optical bowing", was also observed for the nanocrystals. We reported nearly similar observations for homogeneous $Zn_xCd_{1-x}S$ QDs.[17] Room-temperature emission efficiencies ranging from 70 to 85% and spectral widths (fwhm) of 22−30 nm have been achieved for $Zn_xCd_{1-x}Se$ QDs, while efficiencies of 25−50% and very narrow fwhm of 14−18 nm have been reported for QDs of $Zn_xCd_{1-x}S$. These values are comparable to those obtained for CdSe-based nanocrystals. Water-soluble $Zn_xCd_{1-x}Se$ QDs when heated in an air-saturated aqueous solution were found to have high PL stability (much more stable than the CdSe−ZnS core−shell nanostructures), enabling their use in biological applications (e.g., biolabeling and biosensing). Recently, continuous emission has been observed from single nanocrystals of ZnSe-capped $Zn_xCd_{1-x}Se$ having a gradient structure.[43] Their unusual nonblinking property is in stark contrast to individual CdSe-based nanocrystals, whose photoluminescence turns on and off intermittently (Figure 6). These continuously emitting nanocrystals would be very useful in applications that require a continuous output of photons.

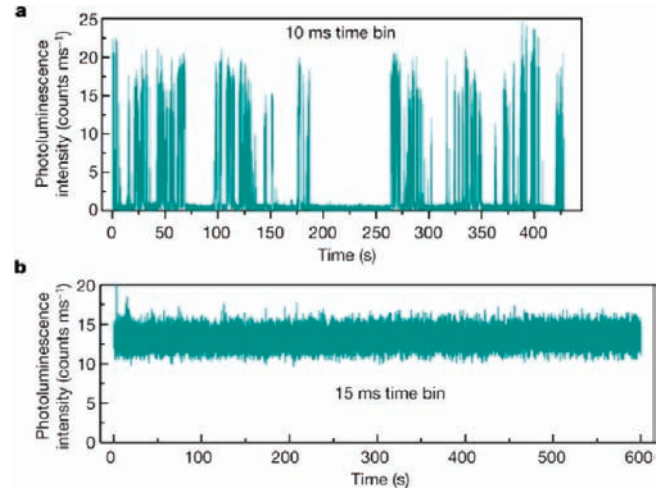

FIGURE 6. Time-dependent photoluminescent intensity traces from a single nanocrystal of (a) CdSe-ZnSe (on-and-off emission) and (b) ZnCdSe-ZnSe (continuous emission). Reprinted with permission from Macmillan Publishers Ltd.: Nature (ref 43), copyright 2009.

In the case of homogeneous $CdE'_xE''_{1-x}$ alloys, the observed optical bowing is more pronounced as can be seen in Figure 7 for both the bulk and the nanocrystal forms of $CdSe_xTe_{1-x}$ alloy.[21] With this strong nonlinear composition effect, certain alloy compositions can emit light at wavelengths that are outside the spectral range defined by the parent binary systems. This is depicted in Figure 7, where nanocrystals of $CdSe_xTe_{1-x}$ are shown to emit light at wavelengths longer than those emitted by their parent binary nanocrystals of similar size. This makes them desirable in the preparation of near-infrared-emitting nanocrystals, which will be discussed in one of the sections below. It is also worth mentioning that the extent of optical bowing is less in gradient alloys than in homogeneous alloys as reported for CdS_xTe_{1-x} nanocrystals.[22]

5.1.1. Short-Wavelength Visible Emission. By tuning the size of semiconductor nanocrystals, emission color spanning the entire visible spectrum has been achieved. However, as in the case of the widely studied CdSe nanocrystals, the extremely small particles (<2 nm) needed to produce emission in the short-wavelength visible spectral region are not very stable and are difficult to passivate, and this consequently leads to low emission efficiencies and broad spectral widths. In contrast, alloying of CdSe and ZnSe to produce composition-tunable $Zn_xCd_{1-x}Se$ nanocrystals has resulted in highly luminescent and stable green- and blue-emitting materials.[11,12,44] The high stability of these alloyed nanocrystals is

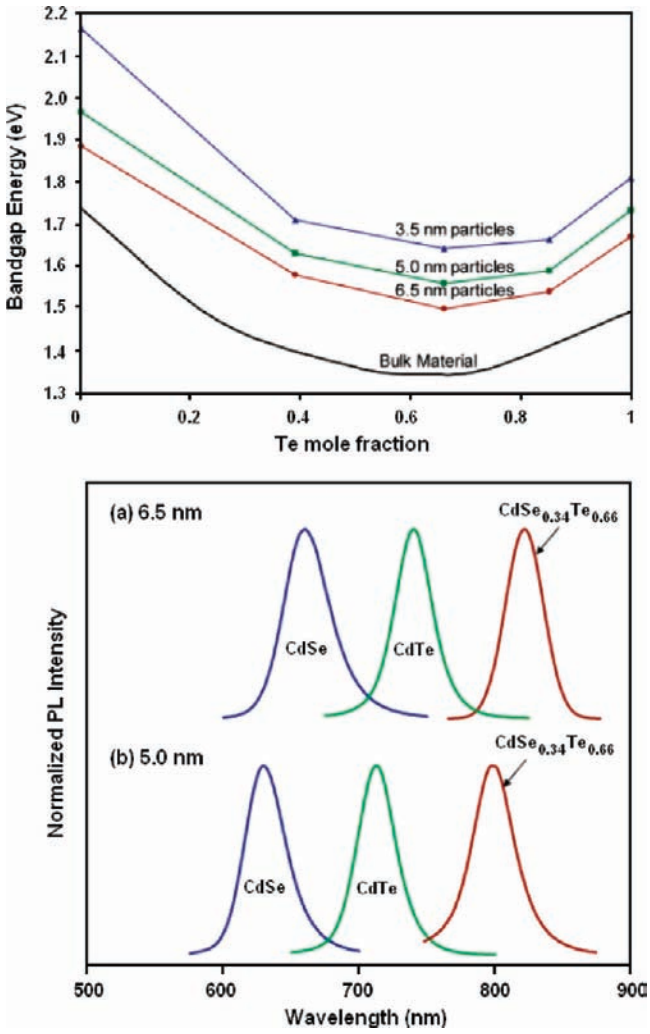

FIGURE 7. Top: Composition dependence of the band gap energy for bulk and nanocrystalline $CdSe_xTe_{1-x}$ alloy. Bottom: Comparison of the emission spectra among CdSe, CdTe, and $CdSe_{0.34}Te_{0.66}$ nanocrystals with similar overall diameter of (a) 6.5 nm and (b) 5.0 nm. Adapted with permission from ref 21. Copyright 2003 American Chemical Society.

primarily attributed to their larger size (e.g., blue-emitting $Zn_xCd_{1-x}Se$ nanocrystals have particle sizes that are 2−3 times larger than those of the blue-emitting CdSe-ZnS core−shell nanostructures). Figure 8 shows $Zn_xCd_{1-x}Se$ nanocrystals, whose composition is tuned to emit colors in the blue-green spectral range. These materials should be excellent for short-wavelength optoelectronic devices and can also be utilized in white-light generation. Alloyed $Zn_xCd_{1-x}S$ nanocrystals have also been shown to emit blue light with high efficiency.[45] Using ZnS-capped $Zn_xCd_{1-x}S$ quantum dots, Bae et al. were able to fabricate deep blue light-emitting diodes.[46]

5.1.2. NIR Emission. The near-infrared (NIR) spectral window (700−1400 nm) has been increasingly important in the areas of biomedical imaging and detection, telecommunication, as well as photovoltaics. This has triggered several studies of semiconductor nanocrystals that can efficiently absorb and emit light in the NIR region. Jiang et al. have optimized the synthetic conditions for the preparation of CdS-capped $CdSe_xTe_{1-x}$ QDs that exhibit emission wavelengths ranging from 600 to 850 nm.[26] These QDs have been found to have good PL properties and high resistance against photobleaching. Moreover, they have conjugated these QDs to biorecognition molecules and demonstrated their use in multiplexed imaging and biolabeling. Pons et al., on the other hand, have coated $CdSe_xTe_{1-x}$ QDs with ~3 monolayers of oxidation-resistant ZnCdS shell, producing NIR-emitting QDs that are highly stable in a wide range of salinity.[27] Water-soluble core−shell−shell QDs having $InAs_xP_{1-x}$ core have been utilized in NIR sentinel lymph node (SLN) mapping experiments.[36] When injected intradermally into the paw of a mouse, these QDs enter the lymphatics and migrate to the SLN within a minute, as seen using an intraoperative imaging system. Gradiently alloyed $Cd_xHg_{1-x}Te$ nanocrystals have been incorporated into a polymer matrix.[30] The resulting nanocrystal−polymer bulk composites exhibited intense PL emission that is tunable from 1100 to 1400 nm, which makes them potentially useful in optical communications. Also, $Cd_xHg_{1-x}Te$ nanocrystals emitting at 750−1200 nm have been used to label biocompatible polymer microcapsules, which shows promise for monitoring drug delivery processes.[47] Meanwhile, CdS-capped $Cd_xHg_{1-x}Te$ nanocrystals that emit at 790 nm have been successfully used for in vivo imaging of a living mouse (Figure 9).[31]

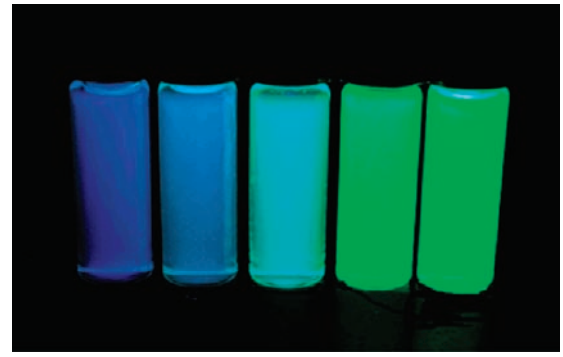

FIGURE 8. Blue and green emission of composition-tunable $Zn_xCd_{1-x}Se$ nanocrystals. Reprinted with permission from ref 11. Copyright 2004 American Chemical Society.

5.1.3. Ion Sensor Applications. The superior luminescence properties exhibited by alloyed nanocrystals have allowed their use in sensing applications. Ali et al. have explored the utility of glutathione-capped $Zn_xCd_{1-x}Se$ QDs as fluorescent Pb^{2+} sensor.[48] The probe displays high sensitivity (detection limit of 20 nM) and high selectivity toward Pb^{2+} in the presence of other metal ions. Moreover, it was found to

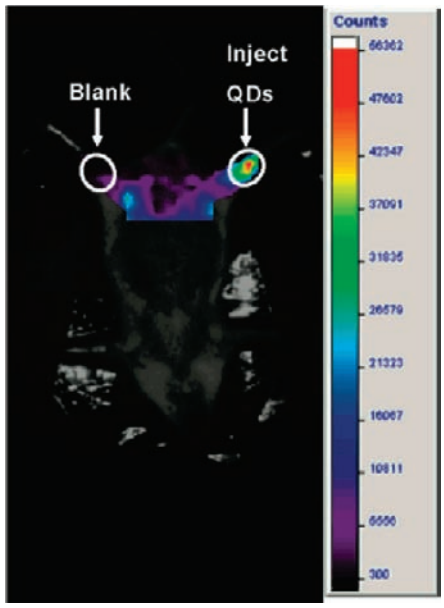

FIGURE 9. Fluorescence in vivo image of a live mouse after injection of CdS-capped $Cd_xHg_{1-x}Te$ nanocrystals into its right leg. Reprinted with permission from ref 31. Copyright 2007 American Chemical Society.

have better sensitivity than glutathione-capped CdSe QDs of the same size. Liu et al., on the other hand, have demonstrated the use of glutathione-capped $Zn_xHg_{1-x}Se$ QDs for sensitive and selective detection of Cu^{2+} ions.[33]

5.2. Solar Cell Applications. Several size-tunable binary nanocrystals have been explored for photovoltaic devices, but the poor charge transport between very small nanocrystals results in low efficiencies. Employing composition-tunable alloyed nanocrystals will enable us to make use of quantum confinement effects in improving the optical absorption process without overly impeding the subsequent transport of charge to the electrodes. Pb chalcogenides have been extensively investigated for nanocrystal-based solar cells because of their narrow band gap (ideal for NIR absorption) and large excitonic Bohr radius (provides access to the strong confinement limit).[49] Solar cells containing PbSe nanocrystals have been found to exhibit large short-circuit photocurrent densities (J_{SC}), while those with nanocrystalline PbS have shown large open-circuit voltages (V_{OC}).[50] With the creation of photovoltaic cells containing nanocrystalline PbS_xSe_{1-x} alloy, an enhancement in both J_{SC} and V_{OC} was realized, resulting in higher power conversion efficiency relative to those of the constituent binary systems.[35]

The chalcopyrite-based semiconductors are another class of materials that are utilized in the fabrication of photovoltaic cells. Schulz et al. demonstrated the use of nanoparticle-based spray deposition technique in the development of small-area CIGS solar cells.[37] Guo et al., on the other hand, have fabricated $Cu(In_{1-x}Ga_x)(S_{1-y}Se_y)_2$ photovoltaic absorber films through selenization of $CuIn_xGa_{1-x}S_2$ nanocrystals.[39] Although further studies are needed to improve the device performance of nanocrystal-derived absorber films, the nonvacuum nanocrystal-based processes have shown great promise as a simple, low-cost, and easily scalable method in the production of thin film solar cells.

6. Conclusion and Perspectives

A summary of recent studies on alloyed semiconductor nanocrystals has been provided in this Account. The growing interest in these nanomaterials is primarily due to the unique properties that emerge upon alloying of two binary or two ternary semiconductors, allowing their use in optoelectronics, photovoltaics, and biomedical and sensing applications. As research on alloyed nanocrystals is still in its infancy, many of the materials properties and potential uses are yet to be discovered. In the next few years, we expect an increase in the number of publications on these nanoscale alloys that report on properties other than their most often studied optical properties. For instance, colloidal alloyed semiconductor nanocrystals with composition-tunable magnetic properties have not yet been investigated. It has been previously reported that the ferromagnetic ordering temperature of semiconducting EuS can be tuned by altering the band gap via control of particle size.[51] However, the extremely small bulk exciton Bohr radius of EuS ($r \sim 1.2$ nm) and the difficulty in preparing high-quality nanoparticles that are less than 2 nm in diameter have prevented access to the strong confinement regime, where the effects of quantum confinement are more pronounced. Also, magnetic nanoparticles of very small size usually exhibit superparamagnetism. Thus, it would be interesting to know how the magnetic properties will change upon alloying ferromagnetic EuS ($E_g = 1.65$ eV) with wider band gap europium chalcogenides, such as metamagnetic EuSe ($E_g = 1.80$ eV) and antiferromagnetic EuTe ($E_g = 2.00$ eV), at the nanoscale. Moreover, alloying of semiconducting EuS and metallic GdS may also result in alloyed nanocrystals with interesting electronic and magnetic properties.

Although many of the synthetic approaches that are summarized in this Account have been successful in producing high-quality colloidal alloyed nanocrystals, several issues remain to be resolved. For example, there is still a need to distinguish the optimum synthetic parameters for preparing gradiently alloyed nanocrystals from those used in producing nanocrystalline homogeneous alloys having the same components. To achieve this, it is important to have a deeper understanding of the mechanism involved in nanoalloy for-

mation. Also, to enable the widespread commercialization of nanoalloy-based devices, it is necessary to design synthetic procedures that will allow for large-scale production of these nanomaterials.

BIOGRAPHICAL INFORMATION

Michelle D. Regulacio received her Ph.D. in Chemistry from Georgetown University under the mentorship of Dr. Sarah L. Stoll. She spent 1 year as a postdoctoral research associate in the lab of Dr. Robert J. Cava at Princeton University before joining the Institute of Materials Research and Engineering in Singapore as a research engineer. Aside from alloyed nanocrystals, her research interests include magnetic nanoparticles, lanthanide luminescence, and superconducting materials.

Ming-Yong Han obtained his Ph.D. in Chemistry from Jilin University. He was with IBM and Indiana University before his current joint appointment as senior scientist with the Institute of Materials Research and Engineering and National University of Singapore. His research addresses problems at the interfaces of nanoscience, nanotechnology, biotechnology, and optoelectronics. He has more than 20 granted patents and pending applications.

FOOTNOTES

*To whom correspondence should be addressed. E-mail: my-han@imre.a-star.edu.sg.

REFERENCES

1 Steigerwald, M. L.; Brus, L. E. Semiconductor Crystallites - A Class of Large Molecules. *Acc. Chem. Res.* **1990**, *23*, 183–188.

2 Trindade, T. Nanocrystalline Semiconductors: Synthesis, Properties, and Perspectives. *Chem. Mater.* **2001**, *13*, 3843–3858.

3 Murray, C. B.; Norris, D. J.; Bawendi, M. G. Synthesis and characterization of nearly monodisperse CdE (E = sulfur, selenium, tellurium) semiconductor nanocrystallites. *J. Am. Chem. Soc.* **1993**, *115*, 8706–8715.

4 Beaulac, R.; Archer, P. I.; Gamelin, D. R. Luminescence in colloidal Mn^{2+}-doped semiconductor nanocrystals. *J. Solid State Chem.* **2008**, *181*, 1582–1589.

5 Zhong, X. H.; Han, M. Y.; Dong, Z. L.; White, T. J.; Knoll, W. Composition-tunable $Zn_xCd_{1-x}Se$ nanocrystals with high luminescence and stability. *J. Am. Chem. Soc.* **2003**, *125*, 8589–8594.

6 Deng, Z.; Yan, H.; Liu, Y. Band Gap Engineering of Quarternary-Alloyed ZnCdSSe Quantum Dots via a Facile Phosphine-Free Colloidal Method. *J. Am. Chem. Soc.* **2009**, *131*, 17744–17745.

7 Tang, J.; Hinds, S.; Kelley, S. O.; Sargent, E. H. Synthesis of Colloidal $CuGaSe_2$, $CuInSe_2$, and $Cu(InGa)Se_2$ Nanoparticles. *Chem. Mater.* **2008**, *20*, 6906–6910.

8 Pan, D. C.; Weng, D.; Wang, X. L.; Xiao, Q. F.; Chen, W.; Xu, C. L.; Yang, Z. Z.; Lu, Y. F. Alloyed semiconductor nanocrystals with broad tunable band gaps. *Chem. Commun.* **2009**, *xxx*, 4221–4223.

9 Heiba, Z. K.; Arda, L. Structural properties of $Zn_{1-x}Mg_xO$ nanomaterials prepared by sol-gel method. *Cryst. Res. Technol.* **2009**, *44*, 845–850.

10 Yin, Y.; Alivisatos, A. P. Colloidal nanocrystal synthesis and the organic-inorganic interface. *Nature* **2005**, *437*, 664–670.

11 Zhong, X. H.; Zhang, Z. H.; Liu, S. H.; Han, M. Y.; Knoll, W. Embryonic nuclei-induced alloying process for the reproducible synthesis of blue-emitting $Zn_xCd_{1-x}Se$ nanocrystals with long-time thermal stability in size distribution and emission wavelength. *J. Phys. Chem. B* **2004**, *108*, 15552–15559.

12 Zhong, X. H.; Feng, Y. Y.; Zhang, Y. L.; Gu, Z. Y.; Zou, L. A facile route to violet- to orange-emitting $Cd_xZn_{1-x}Se$ alloy nanocrystals via cation exchange reaction. *Nanotechnology* **2007**, *18*, 385606.

13 Zheng, Y. G.; Yang, Z. C.; Ying, J. Y. Aqueous synthesis of glutathione-capped ZnSe and $Zn_{1-x}Cd_xSe$ alloyed quantum dots. *Adv. Mater.* **2007**, *19*, 1475–1479.

14 Liu, F. C.; Cheng, T. L.; Shen, C. C.; Tseng, W. L.; Chiang, M. Y. Synthesis of cysteine-capped $Zn_xCd_{1-x}Se$ alloyed quantum dots emitting in the blue-green spectral range. *Langmuir* **2008**, *24*, 2162–2167.

15 Protiere, M.; Reiss, P. Highly luminescent $Cd_{1-x}Zn_xSe/ZnS$ core shell nanocrystals emitting in the blue-green spectral range. *Small* **2007**, *3*, 399–403.

16 Wang, W. Z.; Germanenko, I.; El-Shall, M. S. Room-temperature synthesis and characterization of nanocrystalline CdS, ZnS, and $Cd_xZn_{1-x}S$. *Chem. Mater.* **2002**, *14*, 3028–3033.

17 Zhong, X. H.; Feng, Y. Y.; Knoll, W.; Han, M. Y. Alloyed $Zn_xCd_{1-x}S$ nanocrystals with highly narrow luminescence spectral width. *J. Am. Chem. Soc.* **2003**, *125*, 13559–13563.

18 Li, Y. C.; Ye, M. F.; Yang, C. H.; Li, X. H.; Li, Y. F. Composition- and shape-controlled synthesis and optical properties of $Zn_xCd_{1-x}S$ alloyed nanocrystals. *Adv. Funct. Mater.* **2005**, *15*, 433–441.

19 Ouyang, J. Y.; Ratcliffe, C. I.; Kingston, D.; Wilkinson, B.; Kuijper, J.; Wu, X. H.; Ripmeester, J. A.; Yu, K. Gradiently alloyed $Zn_xCd_{1-x}S$ colloidal photoluminescent quantum dots synthesized via a noninjection one-pot approach. *J. Phys. Chem. C* **2008**, *112*, 4908–4919.

20 Swafford, L. A.; Weigand, L. A.; Bowers, M. J.; McBride, J. R.; Rapaport, J. L.; Watt, T. L.; Dixit, S. K.; Feldman, L. C.; Rosenthal, S. J. Homogeneously alloyed CdS_xSe_{1-x} nanocrystals: Synthesis, characterization, and composition/size-dependent band gap. *J. Am. Chem. Soc.* **2006**, *128*, 12299–12306.

21 Bailey, R. E.; Nie, S. M. Alloyed semiconductor quantum dots: Tuning the optical properties without changing the particle size. *J. Am. Chem. Soc.* **2003**, *125*, 7100–7106.

22 Gurusinghe, N. P.; Hewa-Kasakarage, N. N.; Zamkov, M. Composition-tunable properties of CdS_xTe_{1-x} alloy nanocrystals. *J. Phys. Chem. C* **2008**, *112*, 12795–12800.

23 Al-Salim, N.; Young, A. G.; Tilley, R. D.; McQuillan, A. J.; Xia, J. Synthesis of CdSeS nanocrystals in coordinating and noncoordinating solvents: Solvent's role in evolution of the optical and structural properties. *Chem. Mater.* **2007**, *19*, 5185–5193.

24 Piven, N.; Susha, A. S.; Doeblinger, M.; Rogach, A. L. Aqueous synthesis of alloyed $CdSe_xTe_{1-x}$ nanocrystals. *J. Phys. Chem. C* **2008**, *112*, 15253–15259.

25 Ouyang, J. Y.; Vincent, M.; Kingston, D.; Descours, P.; Boivineau, T.; Zaman, M. B.; Wu, X. H.; Yu, K. Noninjection, One-Pot Synthesis of Photoluminescent Colloidal Homogeneously Alloyed CdSeS Quantum Dots. *J. Phys. Chem. C* **2009**, *113*, 5193–5200.

26 Jiang, W.; Singhal, A.; Zheng, J. N.; Wang, C.; Chan, W. C. W. Optimizing the synthesis of red- to near-IR-emitting CdS-capped $CdTe_xSe_{1-x}$ alloyed quantum dots for biomedical imaging. *Chem. Mater.* **2006**, *18*, 4845–4854.

27 Pons, T.; Lequeux, N.; Mahler, B.; Sasnouski, S.; Fragola, A.; Dubertret, B. Synthesis of Near-Infrared-Emitting, Water-Soluble CdTeSe/CdZnS Core/Shell Quantum Dots. *Chem. Mater.* **2009**, *21*, 1418–1424.

28 Li, Y. C.; Zhong, H. Z.; Li, R.; Zhou, Y.; Yang, C. H.; Li, Y. F. High-yield fabrication and electrochemical characterization of tetrapodal CdSe, CdTe, and $CdSe_xTe_{1-x}$ nanocrystals. *Adv. Funct. Mater.* **2006**, *16*, 1705–1716.

29 Rogach, A. L.; Harrison, M. T.; Kershaw, S. V.; Kornowski, A.; Burt, M. G.; Eychmuller, A.; Weller, H. Colloidally Prepared CdHgTe and HgTe Quantum Dots with Strong Near-Infrared Luminescence. *Phys. Status Solidi B* **2001**, *224*, 153–158.

30 Sun, H. Z.; Zhang, H.; Ju, J.; Zhang, J. H.; Qian, G.; Wang, C. L.; Yang, B.; Wang, Z. Y. One-Step Synthesis of High-Quality Gradient CdHgTe Nanocrystals: A Prerequisite to Prepare CdHgTe-Polymer Bulk Composites with Intense Near-Infrared Photoluminescence. *Chem. Mater.* **2008**, *20*, 6764–6769.

31 Qian, H.; Dong, C.; Peng, J.; Qiu, X.; Xu, Y.; Ren, J. High-quality and water-soluble near-infrared photoluminescent CdHgTe/CdS quantum dots prepared by adjusting size and composition. *J. Phys. Chem. C* **2007**, *111*, 16852–16857.

32 Tsay, J. M.; Pflughoefft, M.; Bentolila, L. A.; Weiss, S. Hybrid approach to the synthesis of highly luminescent CdTe/ZnS and CdHgTe/ZnS nanocrystals. *J. Am. Chem. Soc.* **2004**, *126*, 1926–1927.

33 Liu, F. C.; Chen, Y. M.; Lin, J. H.; Tseng, W. L. Synthesis of highly fluorescent glutathione-capped $Zn_xHg_{1-x}Se$ quantum dot and its application for sensing copper ion. *J. Colloid Interface Sci.* **2009**, *337*, 414–419.

34 Arachchige, I. U.; Kanatzidis, M. G. Anomalous Band Gap Evolution from Band Inversion in $Pb_{1-x}Sn_xTe$ Nanocrystals. *Nano Lett.* **2009**, *9*, 1583–1587.

35 Ma, W.; Luther, J. M.; Zheng, H. M.; Wu, Y.; Alivisatos, A. P. Photovoltaic Devices Employing Ternary PbS_xSe_{1-x} Nanocrystals. *Nano Lett.* **2009**, *9*, 1699–1703.

36 Kim, S. W.; Zimmer, J. P.; Ohnishi, S.; Tracy, J. B.; Frangioni, J. V.; Bawendi, M. G. Engineering $InAs_xP_{1-x}$/InP/ZnSe III-V alloyed core/shell quantum dots for the near-infrared. *J. Am. Chem. Soc.* **2005**, *127*, 10526–10532.

37 Schulz, D. L.; Curtis, C. J.; Flitton, R. A.; Wiesner, H.; Keane, J.; Matson, R. J.; Jones, K. M.; Parilla, P. A.; Noufi, R.; Ginley, D. S. Cu-In-Ga-Se nanoparticle colloids as spray deposition precursors for Cu(In, Ga)Se-2 solar cell materials. *J. Electron. Mater.* **1998**, *27*, 433–437.

38 Panthani, M. G.; Akhavan, V.; Goodfellow, B.; Schmidtke, J. P.; Dunn, L.; Dodabalapur, A.; Barbara, P. F.; Korgel, B. A. Synthesis of $CuInS_2$, $CuInSe_2$, and $Cu(In_xGa_{1-x})Se_2$ (CIGS) Nanocrystal "Inks" for Printable Photovoltaics. *J. Am. Chem. Soc.* **2008**, *130*, 16770–16777.

39 Guo, Q.; Ford, G. M.; Hillhouse, H. W.; Agrawal, R. Sulfide Nanocrystal Inks for Dense $Cu(In_{1-x}Ga_x)(S_{1-y}Se_y)_2$ Absorber Films and Their Photovoltaic Performance. *Nano Lett.* **2009**, *9*, 3060–3065.

40 Pan, D. C.; Wang, X. L.; Zhou, Z. H.; Chen, W.; Xu, C. L.; Lu, Y. F. Synthesis of Quaternary Semiconductor Nanocrystals with Tunable Band Gaps. *Chem. Mater.* **2009**, *21*, 2489–2493.

41 Sung, Y. M.; Lee, Y. J.; Park, K. S. Kinetic analysis for formation of $Cd_{1-x}Zn_xSe$ solid-solution nanocrystals. *J. Am. Chem. Soc.* **2006**, *128*, 9002–9003.

42 Lee, H.; Holloway, P. H.; Yang, H. Synthesis and characterization of colloidal ternary ZnCdSe semiconductor nanorods. *J. Chem. Phys.* **2006**, *125*, 164711.

43 Wang, X. Y.; Ren, X. F.; Kahen, K.; Hahn, M. A.; Rajeswaran, M.; Maccagnano-Zacher, S.; Silcox, J.; Cragg, G. E.; Efros, A. L.; Krauss, T. D. Non-blinking semiconductor nanocrystals. *Nature* **2009**, *459*, 686–689.

44 Lesnyak, V.; Plotnikov, A.; Gaponik, N.; Eychmuller, A. Toward efficient blue-emitting thiol-capped $Zn_{1-x}Cd_xSe$ nanocrystals. *J. Mater. Chem.* **2008**, *18*, 5142–5146.

45 Bae, W. K.; Nam, M. K.; Char, K.; Lee, S. Gram-Scale One-Pot Synthesis of Highly Luminescent Blue Emitting $Cd_{1-x}Zn_xS$/ZnS Nanocrystals. *Chem. Mater.* **2008**, *20*, 5307–5313.

46 Bae, W. K.; Kwak, J.; Lim, J.; Lee, D.; Nam, M. K.; Char, K.; Lee, C.; Lee, S. Deep blue light-emitting diodes based on $Cd_{1-x}Zn_xS$@ZnS quantum dots. *Nanotechnology* **2009**, *20*, 075202.

47 Gaponik, N.; Radtchenko, I. L.; Gerstenberger, M. R.; Fedutik, Y. A.; Sukhorukov, G. B.; Rogach, A. L. Labeling of biocompatible polymer microcapsules with near-infrared emitting nanocrystals. *Nano Lett.* **2003**, *3*, 369–372.

48 Ali, E. M.; Zheng, Y. G.; Yu, H. H.; Ying, J. Y. Ultrasensitive Pb^{2+} detection by glutathione-capped quantum dots. *Anal. Chem.* **2007**, *79*, 9452–9458.

49 Ellingson, R. J.; Beard, M. C.; Johnson, J. C.; Yu, P. R.; Micic, O. I.; Nozik, A. J.; Shabaev, A.; Efros, A. L. Highly efficient multiple exciton generation in colloidal PbSe and PbS quantum dots. *Nano Lett.* **2005**, *5*, 865–871.

50 Luther, J. M.; Law, M.; Beard, M. C.; Song, Q.; Reese, M. O.; Ellingson, R. J.; Nozik, A. J. Schottky Solar Cells Based on Colloidal Nanocrystal Films. *Nano Lett.* **2008**, *8*, 3488–3492.

51 Regulacio, M. D.; Kar, S.; Zuniga, E.; Wang, G.; Dollahon, N. R.; Yee, G. T.; Stoll, S. L. Size-Dependent Magnetism of EuS Nanoparticles. *Chem. Mater.* **2008**, *20*, 3368–3376.